1-1-2009

Two-photon photodetector in a multiquantum well GaAs laser structure at 1.55 mu m

D. Duchesne

L. Razzari

L. Halloran

R. Morandotti

A. J. Spring Thorpe

See next page for additional authors

Two-photon photodetector in a multiquantum well GaAs laser structure at 1.55μm

D. Duchesne,[1] L. Razzari,[1,2] L. Halloran,[1] R. Morandotti,[1] A. J. SpringThorpe,[3] D. N. Christodoulides,[4] and D. J. Moss[1,5,*]

[1]INRS-EMT, Université du Québec, Varennes, Quebec J3X 1S2, Canada
[2]Dipartimento di Elettronica, Università di Pavia, via Ferrata 1, 27100 Pavia, Italy
[3]Canadian Photonics Fabrication Centre (CPFC), National Research Council of Canada, Ottawa, Ontario K1A 0R6, Canada
[4]College of Optics and Photonics, CREOL & FPCE, University of Central Florida, Florida, Orlando 32816, USA
[5]CUDOS, School of Physics, University of Sydney, Sydney, NSW 2006, Australia
[*]Corresponding author: dmoss@physics.usyd.edu.au

Abstract: We report two-photon photocurrent in a GaAs/AlGaAs multiple quantum well laser at 1.55μm. Using 1ps pulses, a purely quadratic photocurrent is observed. We measure the device efficiency, sensitivity, as well as the two-photon absorption coefficient. The results show that the device has potential for signal processing, autocorrelation and possibly two-photon source applications at sub-Watt power levels.

OCIS codes: (230.4320) Nonlinear optical devices; (040.4200) Multiple quantum well; (230.5170) Photodetectors; (190.4180) Multiphoton processes

References and links

1. F. Liu, K. M. Yoo, and R. R. Alfano, "Ultrafast laser pulse transmission and imaging through biological tissues," Appl. Opt. **32**, 554-558 (1993).
2. P. Xi, Y. Andegeko, L. R. Weisel, V. V. Lozovoy, and M. Dantus, "Greater signal, increased depth, and less photobleaching in two-photon microscopy with 10 fs pulses," Opt. Commun. **281**, 1841-1849 (2008).
3. R. Huber, A. Brodschelm, F. Tauser, and A. Leitenstorfer, "Generation and field-resolved detection of femtosecond electromagnetic pulses tunable up to 41 THz," Appl. Phys. Lett. **76**, 3191-3193 (2000).
4. S. T. Cundiff and J. Ye, "Colloquium: Femtosecond optical frequency combs," Rev. Mod. Phys. **75**, 325-342 (2003).
5. J. K. Ranka, A. L. Gaeta, A. Baltuska, M. S. Pshenichnikov, and D. A. Wiersma, "Autocorrelation measurement of 6-fs pulses based on the two-photon-induced photocurrent in a GaAsP photodiode," Opt. Lett. **22**, 1344-1346 (1997).
6. S. Radic, D. J. Moss, and B. J. Eggleton, "Nonlinear Optics in Communications: From Crippling Impairment to Ultrafast Tools," in *Optical Fiber Telecommunications V: Components and Sub-systems*, I. P. Kaminow, T. Li, and A. E. Willner, ed. (Academic Press, Oxford, UK, 2008), Chap. 20.
7. P. J. Maguire, L. P. Barry, T. Krug, W. H. Guo, J. O'Dowd, M. Lynch, A. L. Bradley, J. F. Donegan and H. Folliot, "Optical signal processing via two-photon absorption in a semiconductor microcavity for the next generation of high-speed optical communications network," J. Lightwave Technol. **24**, 2683-2692 (2006).
8. C. Dorrer, "High-speed measurements for optical telecommunication systems," IEEE J. Sel. Top. Quantum Electron. **12**, 843-858 (2006).
9. S. Wielandy, M. Fishteyn, and B. Zhu, "Optical performance monitoring using nonlinear detection," J. Lightwave Technol. **22**, 784-793 (2004).
10. H. K. Tsang, R. S. Grant, R. V. Penty, I. H. White, J. B. D. Soole, E. Colas, H. P. Leblanc, N. C. Andreadakis, M. S. Kims and W. Sibbett, "GaAs/GaAlAs multiquantum well waveguides for all-optical switching at 1.55 μm," Electron. Lett. **27**, 1993-1995 (1991).
11. Z. Zheng, A. M. Weiner, J. H. Marsh, and M. M. Karkhanehchi, "Ultrafast optical thresholding based on two-photon absorption GaAs waveguide photodetectors," IEEE Photon. Technol. Lett. **9**, 493-495 (1997).
12. R. Salem, M. A. Foster , A. C. Turner, G. F. Geraghty, M. Lipson, and A. L. Gaeta, "Signal regeneration using low-power four-wave mixing on silicon chip," Nat. Photonics **2**, 35-38 (2008).
13. Y. Takagi, T. Kobayashi, K. Yoshihara, and S. Imamura, "Multiple-shot and single-shot sutocorrelator based on 2-photon conductivity in semiconductors," Opt. Lett. **17**, 658-660 (1992).
14. F. R. Laughton, J. H. Marsh, and A. H. Kean, "Very sensitive two-photon absorption GaAs/AlGaAs waveguide detector for an autocorrelator," Electron. Lett. **28**, 1663-1665 (1992).
15. F. R. Laughton, J. H. Marsh, D. A. Barrow, and E. L. Portnoi, "The two-photon absorption semiconductor waveguide autocorrelator," IEEE J. Quantum Electron. **30**, 838-845 (1994).

#106401 - $15.00 USD Received 15 Jan 2009; revised 13 Mar 2009; accepted 16 Mar 2009; published 19 Mar 2009

16. H. K. Tsang, L. Y. Chan, J. B. D. Soole, H. P. LeBlanc, M. A. Koza, and R. Bhat, "High sensitivity autocorrelation using two-photon absorption in InGaAsP waveguides," Electron. Lett. **31**, 1773-1775 (1995).
17. H. Schneider, T. Maier, H. C. Liu, and M. Walther, "Two-photon photocurrent autocorrelation using intersubband transitions at nearly-resonant excitation," Opt. Express **16**, 1523-1528 (2008).
18. F. Chatenoud, K. Dzurko, M. Dion, D. J. Moss, R. Barber, and D. Landheer, "GaAs/AlGaAs multiple quantum well lasers for monolithic integration with optical modulators," Can. J. Phys. **69**, 491-496 (1991).
19. D. Moss, F. Chatenoud, S. Charbonneau, A. Delage, D. Landheer, and R. Barber, "Laser compatible waveguide modulators," Can. J. Phys. **69**, 497-507 (1991).
20. D. J. Moss, D. Landheer, D. Halliday, S. Charbonneau, R. Barber, F. Chatenoud and D. Conn, "High speed photodetection in a reverse biased GaAs/AlGaAs GRINSCH SQW laser structure," Photon. Technol. Lett. **4**, 609-611 (1992).
21. D. Moss, D. Landheer, A. Delage, F. Chatenoud, and M. Dion, "Laser compatible waveguide electroabsorption modulator with high contrast and low operating voltage in GaAs/AlGaAs," IEEE Photon. Technol. Lett. **3**, 645-647 (1991).
22. A. M. Fox, D. A. B. Miller, G. Livescu, J. E. Cunningham and W. Y. Jan, "Quantum-well carrier sweep out - relation to electroabsorption and exciton saturation," IEEE J. Quantum Electron. **27**, 2281-2295 (1991).
23. T. H. Wood, J. Z. Pastalan, C. A. Burrus, Jr., B. C. Johnson, B. I. Miller, J. L. deMiguel, U. Koren and M. G. Young, "Electric-field screening by photogenerated holes in multiple quantum wells - A new mechanism for absorption saturation," Appl. Phys. Lett. **57**, 1081-1083 (1990).
24. D. J. Moss, T. Ido, and H. Sano, "Calculation of photogenerated carrier escape times in GaAs/AlGaAs quantum wells," IEEE J. Quantum Electron. **30**, 1015-1026 (1994).
25. D. P. Halliday, D. Moss, S. Charbonneau, G. Aers, F. Chatenoud, and D. Landheer, "Time resolved photo luminescence studies in a reverse biased QW laser structure," Appl. Phys. Lett. **61**, 2497-2499 (1992).
26. T. Ido, H. Sano, S. Tanaka, D. J. Moss, and H. Inoue, "Performance of strained InGaAs/InAlAs multiple-quantum-well electroabsorption modulators," IEEE J. Lightwave Technol. **14**, 2324 -2331 (1996).
27. T. Ido, H. Sano, D. J. Moss, S. Tanaka and A. Takai, "Strained InGaAs/InAlAs MQW electroabsorption modulators with large bandwidth and low driving voltage," IEEE Photon. Technol. Lett. **6**, 1207-1209 (1994).
28. D. J. Moss, T. Ido, and H. Sano, "Photogenerated carrier sweep out times in strained $In_xGa_{1-x}As/In_yAs_{1-y}As$ quantum well waveguide modulators at λ=1.55 μm," Electron. Lett. **30**, 405-406 (1994).
29. D. J. Moss, M. Aoki, and H. Sano, "Comparison of photoconductive response times of InGaAs/InAlAs and InGaAs/InGaAsP MQW waveguide modulators," Jpn. J. Appl. Phys. **33,** 328-330 (1994).
30. J. S. Aitchison, D. C. Hutchings, J. U. Kang, G. I. Stegeman, and A. Villeneuve, "The nonlinear optical properties of AlGaAs at the half band gap," IEEE J. Quantum Electron. **33**, 341-348 (1997).
31. A. Villeneuve, C. C. Yang, G. I. Stegeman, C. N. Ironside, G. Scelsi, and R. M. Osgood, "Nonlinear absorption in a GaAs waveguide just above half the band gap," IEEE J. Quantum Electron. **30**, 1172-1175 (1994).
32. H. M. van Driel, "Semiconductor optics - On the path to entanglement," Nat. Photononics **2**, 212-213 (2008).
33. A. Larsson, P. A. Andrekson, S. T. Eng and A. Yariv, "Tunable superlattice p-i-n photodetectors: characteristics, theory, and applications," IEEE J. Quantum Electron. **24**, 787-801 (1988).
34. N. Holonyak, R. M. Kolbas, R. D. Dupuis and P. D. Dapkus, "Quantum-well heterostructure lasers," IEEE. J. Quantum Electron. **16**, 170-186 (1980).
35. A. Yariv and P. Yeh, *Photonics: optical electronics in modern communications*, (Oxford University Press, New York, 2006).
36. D. A. B. Miller, D. S. Chemla, T. C. Damen, A. C. Gossard, W. Wiegmann, T. H. Wood and C. A. Burrus, "Band-edge elecroabsorption in quantum well structures: the quantum confined stark effect," Phys. Rev. Lett. **53**, 2173-2176 (1984).
37. M. N. Islam, C. E. Soccolich, R. E. Slusher, A. F. J. Levi, W. S. Hobson and M. G. Young, "Nonlinear spectroscopy near half-gap in bulk and quantum well GaAs/AlGaAs waveguides," J. Appl. Phys. **71,** 1927-1935 (1992).
38. A. D. Lad, P. P. Kiran, D. More, G. R. Kumar, and S. Mahamuni, "Two-photon absorption in ZnSe and ZnSe/ZnS core/shell quantum structures," Appl. Phys. Lett. **92**, 043126 (2008).
39. H.-S. Chen, S.-L. Liu, and C. C. Yang, "Enhancement of multi-photon processes with carrier injection in a GaAs/AlGaAs quantum well laser structure," Opt. Commun. **235**, 163-167 (2004).
40. A. Shimizu, T. Ogawa and H. Sakaki, "Two-photon absorption spectra of quasi-low-dimensional exciton systems," Phys. Rev. B **45**, 11339-11341 (1992).
41. J. B. Khurgin, "Nonlinear response of the semiconductor quantum-confined structures near and below the middle of the bandgap," J. Opt. Soc. Am. B **11**, 624-631 (1994).
42. H. Folliot, M. Lynch, A. L. Bradley, T. Krug, L. A. Dunbar, J. Hegarty, and J. F. Donegan and L. P. Barry, "Two-photon-induced photoconductivity enhancement in semiconductor microcavities: a theoretical investigation," J. Opt. Soc. Am. B **19**, 2396-2402 (2002).
43. F. R. Laughton, J. H. Marsh and J. S. Roberts, "Intuitive model to include the effect of free-carrier absorption in calculating the two-photon absorption coefficient," Appl. Phys. Lett. **60**, 166-168 (1992).
44. A. Villeneuve, C. C. Yang, G. I. Stegeman, C.-H. Lin, and H.-H. Lin, "Nonlinear refractive-index and two photon-absorption near half the band gap in AlGaAs," Appl. Phys. Lett. **62**, 2465-2467 (1993).

#106401 - $15.00 USD Received 15 Jan 2009; revised 13 Mar 2009; accepted 16 Mar 2009; published 19 Mar 2009

45. C. C. Yang, A. Villeneuve, G. I. Stegeman, C.-H. Lin, and H.-H. Lin, "Anisotropic Two-Photon Transitions in GaAs/AlGaAs Multiple Quantum Well Waveguides," IEEE J. Quantum Electron. **29**, 2934-2939 (1993).
46. D. T. Reid, W. Sibbett, J. M. Dudley, L. P. Barry, B. Thomsen, and J. D. Harvey, "Commercial semiconductor devices for two photon absorption autocorrelation of ultrashort light pulses," Opt. Photon. News **9**, 8142-8144 (1998).
47. T. K. Liang, H. K. Tsang, I. E. Day, J. Drake, A. P. Knights, and M. Asghari, "Silicon waveguide two-photon absorption detector at 1.5 μm wavelength for autocorrelation measurements," Appl. Phys. Lett **81**, 1323-1325 (2002).

1. Introduction

Generation and characterization of ultrashort laser pulses have found important applications in fields as different as bio-medical sensing and imaging [1,2], terathertz generation and detection [3], frequency comb synthesis [4], and the general probing of ultrashort interactions or processes [5]. Nonetheless, the characterization of these ultrashort pulses remains a difficult challenge. Current all-optical techniques used to measure pulse durations and profiles in the picosecond regime typically rely on temporal or frequency mapping methods employing nonlinear effects, such as FROG, SPIDER and most commonly simple cross and auto-correlations based on second harmonic generation. Unfortunately, these techniques are often bulky and difficult to implement in an integrated format. As an alternative, two photon detectors were developed and experienced a great deal of interest in the 1990s as efficient measurement tools for sub-picosecond pulses. However, research in this area tapered off around 8 to 10 years ago, paradoxically just as interest in all-optical signal processing gained significant momentum. Today, information processing in the optical domain has the potentiality of greatly reducing the size, cost, energy consumption as well as increasing the speed of network components and routers for ultrahigh bandwidth telecommunications systems at 1550nm [6,7]. Two-photon detectors have been shown to be ideal for optical time division multiplexing [8], optical performance monitoring [9], switching [10], and for optical thresholding devices in code division multiple access [CDMA] systems [11]. They are attractive in that they combine both the (near instantaneous) nonlinear response with a direct conversion to the electrical domain in a small, cost-effective package.

Despite the volume of work on TPA detectors in the 1990s, as well as concurrent work on linear quantum well optoelectronic devices, comparatively little has been done on GaAs Multiple Quantum Well (MQW) waveguides in terms of their potential use as TPA detectors at 1.55 μm. The first two-photon absorption (TPA) based autocorrelators were demonstrated in silicon [12] and GaAsP [13], and later in GaAs/AlGaAs [14,15] and InGaAsP [16]. Most reports of nonlinear devices operating via TPA were in fact either bulk alloys based or MQWs devices exploiting nonlinear attenuation of the beam, rather than photodetection [14,15]. While TPA photocurrent in a MQW AlGaAs waveguide has already been explored, it was either in a limited context to assess the quality factor for all-optical switching [10], or for applications in the mid-infrared [17].

Given the surge in activity in all-optical signal processing in the last 6 to 8 years [6], it is certainly of significant interest to see whether the enhanced performance of the linear GaAs/AlGaAs MQW optoelectronic devices developed in the 1990s [18-20] for operation at ~775 nm also translate into improved performance for nonlinear (two-photon based) operation at 1550nm (i.e., near the half-bandgap). Considerable effort was devoted to reducing photogenerated carrier pileup, an effect that posed a serious limitation to the optical power handling capability of MQW waveguide electro-absorption (EA) modulators. Solving this issue resulted in significant improvement in EA modulator and waveguide detector performances for both short [18-24] and longer IR wavelength (1550nm) based devices [25-28]. In particular, high performance multifunctional optoelectronics components were reported in GaAs. These devices, suitable for monolithic optoelectronic integration, showed excellent performance as high speed photodetectors [20] and high quality electroabsorption modulators (via the quantum confined Stark Effect [19]), as well as good performance as lasers when forward biased [18]. However, to date, these devices have not been investigated in terms of their potential use for nonlinear, or TPA, based photodetection

#106401 - $15.00 USD Received 15 Jan 2009; revised 13 Mar 2009; accepted 16 Mar 2009; published 19 Mar 2009

In this paper, we report the first observation of two-photon photocurrent at 1550nm in a (reverse biased) GaAs / AlGaAs quantum well laser. This device is similar to previous [18] components developed to achieve efficient multifunctional (laser, electroabsorption modulator, photodetector) performance at 850nm. Here, we show that our device also displays similar advantages when operated as a nonlinear photodetector near 1550nm, such as improved quantum efficiency, high speed operation, negligible saturation effects at high intensities due to carrier pileup effects, as well as, of course, the intrinsic multifunctional performance. Because these components operate efficiently both as reverse-biased EA modulators and two photon detectors, they raise the prospect of being able to electrically modulate the TPA coefficient and hence the nonlinear figure of merit (FOM) [29,30] at 1550nm (ie. near half the direct bandgap, as mentioned before) via the quantum confined Stark Effect. Finally, since this MQW laser structure also exhibits good performances as a laser, it may have a potentially interesting application as a two-photon emitter [31] for entangled photon pair generation.

In the following section we review the basic theory and derive the necessary equations and conditions for nonlinear absorption and photocurrent generation. Section 3 discusses the design and fabrication of the MQW waveguide device, and it is followed by the experimental set-up description in section 4. Finally, our experimental results and analysis are presented in section 5.

2. Theory

Quantum well (QW) structures appeared in the 1980's as a result of advances in technological fabrication processes [32,33], soon proving the ability of discretizing and reducing the density of states [34]. As a consequence, QWs can be used to significantly change the absorption spectra when compared with bulk heterostructure devices. The advantage for laser structures was to decrease the linewidth and lasing threshold current density, making structures significantly more efficient [34]. This was also of benefit for modulators, where the quantum confined Stark shift [35] is greatly enhanced. In addition, quantum confinement of excitons can lead to unique properties not observed in bulk, such as excitonic peaks that are not destroyed either by large applied fields, or at by thermal energy (at room temperature), since carriers cannot tunnel through the surrounding barrier layers. Larger nonlinearities (compared to bulk) have been reported [36-38] in confined structures as a result of the enhanced excitonic effects. The theory of carrier dynamics for TPA has been previously presented [39], and a closed form expression has been recently developed [40].

Nonlinear absorption processes arise from the imaginary part of the odd order nonlinear susceptibilities [29], and generally occur at high optical intensities. When the photon energy is greater than half the bandgap, a two-photon process can occur whereby an electron is excited to the conduction band via a 2 step process involving a virtual state [36]. Efficient TPA photocurrent results for photon energies comprised between the bandgap and the half-band gap, ie.,

$$\frac{1}{2}E_g < hf < E_g . \tag{1}$$

For GaAs, the bandgap is ~ 1.42eV, and the TPA bandwidth is therefore ranging from 870 nm to 1740nm. The intensity, I, of a beam traveling in an GaAs waveguide as a function of the propagation distance along the length of the waveguide is given by [30,41]:

$$\frac{dI}{dz} = -\alpha I - \beta I^2 , \tag{2}$$

where $\alpha = \alpha_{SPA} + \alpha_{SC}$ is the linear propagation loss coefficient including single photon absorption (SPA) (α_{SPA}) as a result of band-to-band absorptions, and scattering losses (α_{SC}) in the waveguide. β is the TPA coefficient and z is the propagation direction. Here we have

#106401 - $15.00 USD Received 15 Jan 2009; revised 13 Mar 2009; accepted 16 Mar 2009; published 19 Mar 2009

neglected higher order nonlinear losses, such as three photon absorption, since each successive higher order nonlinear absorption term has a smaller cross-section than the previous one. Two-photon induced free-carrier absorption (FCA) can be accounted for by adding a term to Eq. (2) [42]:

$$\frac{dI}{dz} = -\alpha I - \beta I^2 - \delta I^3 , \tag{3}$$

where δ is a constant factor given by:

$$\delta = \frac{\sigma\beta \int A(t)dt}{2hf\left[1-\exp\left(-\frac{1}{R\tau}\right)\right]} . \tag{4}$$

In the above equation, σ is the FCA cross-section, τ is the free carrier lifetime, R is the laser repetition rate, f is the central frequency of the pulse, h is Planck's constant, and $A(t)$ is the normalized single input pulse intensity as a function of the time t [42]. However, we verified both experimentally and theoretically that FCA contributions to Eq. (3) are negligible and so Eq. (2) can be solved to obtain:

$$I = \frac{\alpha I_0 \exp(-\alpha z)}{\alpha + \beta I_0 (1-\exp(-\alpha z))} , \tag{5}$$

where I_0 is the input intensity. The total loss is $I_0 - I$, although only absorption due to TPA and SPA can contribute to photocurrent. The total intensity change contributing to TPA is thus:

$$\frac{dI_{TPA}}{dz} = \beta I^2 , \tag{6}$$

from which we obtain,

$$I_{TPA} = I_0\left(1-\frac{\exp(-\alpha z)}{F}\right) - \frac{\alpha}{\beta}\ln(F) , \tag{7}$$

where we have defined a dimensionless parameter,

$$F = 1 + \frac{\beta}{\alpha} I_0 (1-\exp(-\alpha z)) . \tag{8}$$

The total absorbed intensity due to SPA will then be,

$$I_{SPA} = \frac{\alpha_{SPA}}{\beta}\ln(F) . \tag{9}$$

Note that SPA may still occur below the bandgap due to mid-gap defect states as well as via phonon assisted excitations [7] although these are usually small. Equation (7) provides information on the useful range of intensities that will produce a nonlinear quadratic photocurrent. At low intensities, $ln(F) \approx F-1$ and so the photocurrent will be dominated by SPA:

$$I_{abs} = I_{SPA} = I_0 \frac{\alpha_{SPA}}{\alpha}(1-\exp(-\alpha z)) . \tag{10}$$

#106401 - $15.00 USD Received 15 Jan 2009; revised 13 Mar 2009; accepted 16 Mar 2009; published 19 Mar 2009

However, total absorption occurs at higher intensity, where it is dominated by TPA. The dynamic range of intensities leading to quadratic photocurrent can be shown to be [41]:

$$\frac{\alpha_{SPA}}{\beta} \le I_o \le \frac{1}{\beta z}. \tag{11}$$

The maximum number of electron-hole pairs formed will simply be equal to the total number of absorbed photons (or half, for TPA). However, note that not all of the electrons can be collected at the output of the device due to recombination, which will result in a reduced device efficiency. Defining the (internal) quantum efficiency as the ratio of electron-hole pairs collected to the absorbed number of photons absorbed in the material we have the following expression relating the photocurrent to the absorbed energy:

$$N_{eh} = \eta \frac{E_{abs}}{hf} \Rightarrow \frac{dN_{eh}}{dt} = \eta \frac{P_{abs}}{hf} \tag{12}$$

$$J = \eta \frac{eP_{abs}}{hf}, \tag{13}$$

where J is the photocurrent, h is the Planck constant, f is the frequency of the photons, P_{abs} is the absorbed power, e the electronic charge and η is the internal quantum efficiency. For a TPA process, Eq. (13) also contains an additional factor of ½. In general, the absorbed power is a combination of both single photon and multi-photon absorption:

$$J = \eta \frac{eP_{SPA}}{hf} + \eta \frac{eP_{TPA}}{2hf}. \tag{14}$$

We have explicitly assumed the same quantum efficiency for the linear and nonlinear processes. One can define an external quantum efficiency, similar to Eq. (13) but replacing the absorbed power with the incident power:

$$\eta_{ext} = \frac{Jhf}{eP_0}. \tag{15}$$

The external quantum efficiency defines the practical (and experimentally measurable) efficiency of the device and is related to the probability that the SPA and TPA processes occur (i.e. β and α_{SPA}). Note that for a TPA device, the external efficiency is not constant, but rather varies linearly with the input power. The power P may be calculated from the intensity I in waveguides by means of the effective area:

$$A_{eff} = \frac{P}{I} = \frac{\left[\iint_{\infty} |E(x,y)|^2 dxdy\right]^2}{\iint_{\infty} |E(x,y)|^4 dxdy}, \tag{16}$$

where E is the electric field modal distribution in the waveguide which can easily be determined with commercial mode solvers. The total absorbed power is then,

$$P_{abs} = A_{eff}\left(I_{SPA} + I_{TPA}\right). \tag{17}$$

We can now use the above equations to relate the TPA photocurrent to the incident power:

#106401 - $15.00 USD Received 15 Jan 2009; revised 13 Mar 2009; accepted 16 Mar 2009; published 19 Mar 2009

$$J = \eta \frac{e}{2hf}\left[P_0\left(1 - \frac{\exp(-\alpha z)}{F}\right) + \frac{A_{eff}\left(\alpha_{SPA} - \alpha_{SC}\right)}{\beta}\ln(F)\right]. \quad (18)$$

The above expression can be solved numerically for the TPA coefficient. The generation of photocurrent is found to be in part a contribution from the linear SPA and the nonlinear TPA process, whereas scattering losses limits the process. If we assume negligible linear losses and absorption, Eq. (18) reduces to:

$$J = \eta \frac{e}{2hf}\frac{\beta z}{A_{eff}} P_0^2, \quad (19)$$

where we have also assumed $\beta I_0 z << 1$. Eq. (19) illustrates the quadratic dependence of the input power on the photocurrent. Lastly, for practical applications an important figure of merit is the device sensitivity [39],

$$S = P_{peak} \cdot P_{avg}, \quad (20)$$

which corresponds to the minimum value of the product between the peak and the average power that the device is capable of measuring. This figure of merit is often used for SHG autocorrelators. For TPA autocorrelators, another sensitivity measure is often used:

$$S_J = \frac{J}{P_{peak} \cdot P_{avg}}, \quad (21)$$

which relates to the strength of the induced photocurrent.

3. Device design and fabrication

The waveguide structure is a multilayer of $Al_xGa_{1-x}As$, as shown in Figs. 1 and 2, and was designed to optimize laser, detector and modulator performance in a unique device at the lasing wavelength of 850nm. GaAs is an ideal material for inducing nonlinear effects given its large third order nonlinearity [29], which is accentuated in waveguides due to a tight modal field confinement arising from the high index contrast. This results in high intensity values (and hence large nonlinear effects) at moderate or even low power levels. The AlGaAs heterostructure was grown via molecular beam epitaxy, precisely controlling the doping and the temperature. A p-i-n junction was formed by p-doping the top side of the device with beryllium and the bottom side (n-doped) with silicon, with a significant effort placed to keep the background doping in the active layer very low in order to allow for the application of large and uniform bias fields (see below). The active layer consists of four GaAs quantum wells of 8nm widths separated by 3.5 nm $Al_{20}Ga_{80}As$ barriers and forms the core region of the waveguide structure. A high quality film morphology was targeted in order to produce better laser and detector performances than those in bulk GaAs/AlGaAs TPA detectors. The waveguide ridge was defined using stepper lithography and patterned with inductively coupled plasma dry etching, resulting in extremely low sidewall roughness, as shown in Fig. 2. The device was finally metalized, annealed and then cleaved into 250 μm long bars.

The key breakthrough of this device is that a high quality laser was grown at a much lower temperature of 550C to 600C, versus 700C for conventional GRINSCH SQW lasers [18]. This allowed us to precisely control the doping profile in order to form a well defined p-i-n structure. In most lasers, the high growth temperature causes significant diffusion of the p-dopant (typically Beryllium) which has high diffusivity. This in turn results in a very high background p-doping in the QW region. For laser operation this is not a problem, and in fact enhances device performance. For reverse biased detectors and modulators, however, this is a serious issue since achieving a uniform field in the QW region is critical. In order to mitigate the effects of this lower growth temperature, the Al content of the waveguide cladding layers

#106401 - $15.00 USD Received 15 Jan 2009; revised 13 Mar 2009; accepted 16 Mar 2009; published 19 Mar 2009

was reduced to 35%, since it is well known that high Al content layers require high growth temperatures to produce good quality morphology [18].

This device was not planarized, as this fabrication step is normally done to reduce device capacitance in linear detectors addressing high speed performance [19], primarily because the ultrafast response in nonlinear photodetectors is accomplished via the nonlinear response itself, with the photocurrent being integrated for most applications such as autocorrelators. We estimate our RC response time to be on the order of 5ns, implying a capacitance of ~ 50pF. The dark, or leakage, current was not explicitly measured. However, it is expected to be similar to previously reported devices [19] that showed very low leakage currents of only 70pA up to -15V bias.

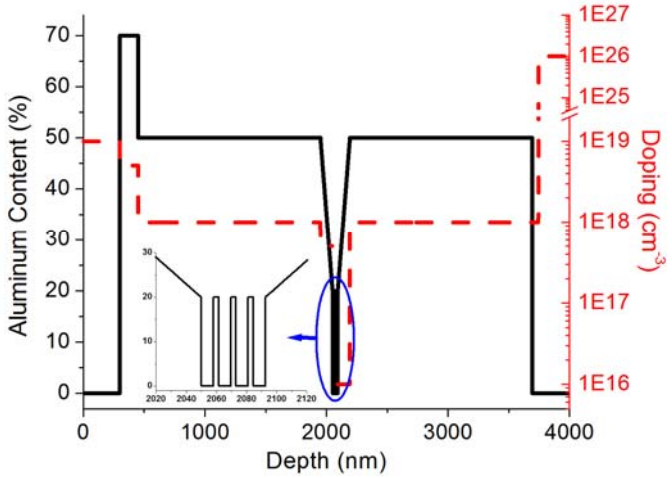

Fig. 1. Doping and alloy profile and of the AlGaAs multilayer structure. Beryllium is used for p-type doping above the quantum wells, and Si is used for n-type doping below. The GaAs substrate is n-doped at 10^{26} cm^{-3}. Inset: Zoom of undoped quantum well region.

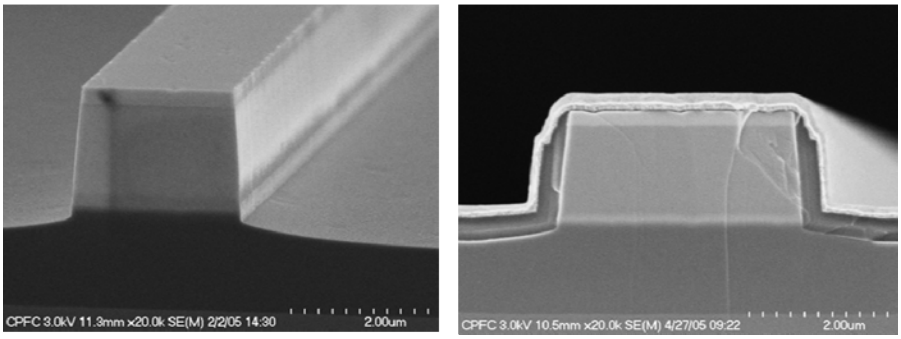

Fig. 2. Scanning electron microscopy pictures of device before (left) and after (right) metallization.

4. Experiment

The waveguide was placed on a three dimensional micro-positioner. Here 50X objectives were used to focus the light onto and out of the device. The beam was passed through an optical chopper and a half-wave plate followed by a polarizer before being coupled into the sample. The output mode could be either imaged by a camera or measured with a power meter and/or a spectrometer. An electrical probe was contacted on top of the device (p-side) and then sent to a lock-in amplifier (operated in current mode) for photogenerated current measurements. Two different laser sources were used in our experiments in order to cover both the linear spectral range of the device at 850 nm, as well as the nonlinear TPA range at 1.55 μm. The low power linear measurements at 850 nm were performed with a tunable 80

#106401 - $15.00 USD Received 15 Jan 2009; revised 13 Mar 2009; accepted 16 Mar 2009; published 19 Mar 2009

MHz Mai Tai oscillator from Spectra Physics operating in a quasi-CW mode. A Pritel fiber laser generating 1ps pulses (measured using a commercial autocorrelator) at 5.19 MHz was used for the nonlinear TPA photocurrent experiment at 1.55 μm. Average power measurements were performed using a photodetector, from which the peak power of our pulses were obtained from the given laser repetition rate and experimentally measured time duration of the pulse. A transverse electric mode polarization was used in all our experiments.

5. Results

5.1 Linear optical characterization

The light intensity-current-voltage test (LIV) of this device, operated under forward bias, is shown in Fig. 3. The threshold current was around 50mA, comparable to similar devices reported previously [18], and somewhat higher than devices optimized solely for laser operation [18] because of the higher series resistance resulting from the very low doping level in the active region.

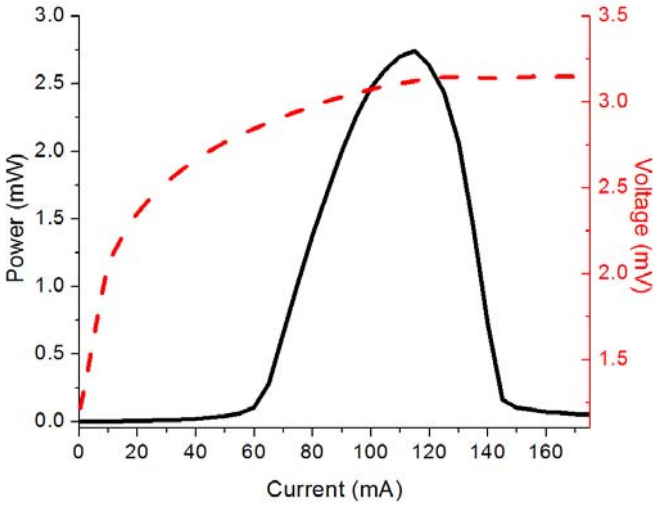

Fig. 3. Light-Current and Voltage-Current curves for the device operated as a laser under forward bias.

Linear optical characterization of the device was performed in the spectral region 840-870nm in order to determine the device absorption edge (i.e. equivalent to the bandgap in continuous media) as well as to check its operation under applied reverse bias fields. The results (shown in Fig. 4) indicate that the absorption edge of the MQW device (under zero bias) is located at ~ 848 nm (1.46 eV), indicating that the half-bandgap is at ~ 1700 nm (0.73 eV). By applying a forward bias, the bandgap shifted to higher energies, whereas a reverse bias resulted in the bandgap shifting to lower energies (i.e., longer wavelengths). The shift in the linear (single photon) band absorption edge of the quantum wells is well understood as the quantum confined Stark Effect (QCSE) [35].

Characterization of the linear optical properties of the device, including transmission and Fabry-Perot fringe measurements, was performed at 1550nm to determine the linear propagation losses. At low CW power levels (sub mW) we observed no noticeable nonlinear transmission or absorption behavior. The propagation loss at 1550nm was measured to be approximately ~ 34.5cm^{-1}. This is primarily a result of the undoped region being much thinner in the current device, resulting in a higher overlap of the waveguide mode with the (lossy) p- and n-doped regions of the cladding layer. In principle this could easily be reduced by increasing the intrinsic layer thickness, with a corresponding increase in the reverse bias voltage (required to achieve the same internal field strength). The dry plasma etching used on the device provided exceptionally low sidewall roughness and high verticality, and so we

#106401 - $15.00 USD Received 15 Jan 2009; revised 13 Mar 2009; accepted 16 Mar 2009; published 19 Mar 2009

expect that the contribution to losses arising from scattering is very low. By using high NA objectives (see previous section) we obtained an estimated coupling efficiency of 50%. As our devices were extremely short, their transmission (considering propagation losses only) is quite high at 42%, whereas the experimental insertion loss of the devices was approximately 13 dB.

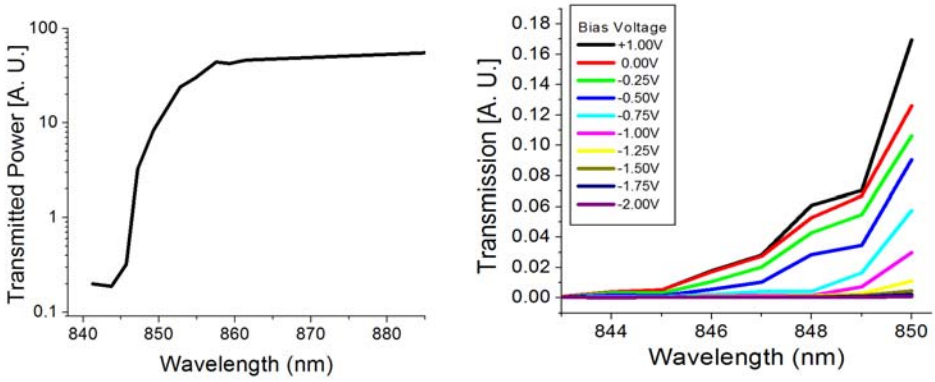

Fig. 4. (left) Linear bandgap measurement and (right) bias-dependant Stark shift.

5.2 Nonlinear optical characterization

Figure 5 shows the average photocurrent from the MQW device at 1550nm with input peak powers ranging from 0 to 10 W. The results are plotted on a log-log scale and the slope of the linear fit is found to be 2.0, indicating a very high adherence to a quadratic response from the TPA process. The negligible single photon absorption contribution to the photocurrent testifies to the excellent growth quality of the device. In fact, the photocurrent remained purely nonlinear for sub-Watt peak powers. Note that the absolute level of absorption of the device is quite low. This is a direct result of the short waveguide length - we estimate that > 200W peak power would be needed to induce a 10% decrease in transmission from TPA alone, which although readily achievable with standard laser sources, would damage the structure. These results suggest that our device is ideal for telecommunication applications where low energy pulses are used, as the pulse can be sampled, monitored or characterized from the effects owing to a strong TPA, while still maintaining an excellent throughput which shows no trace of nonlinear phase or modulation.

The shift in the linear (single photon) band absorption edge of the quantum wells observed in the last section will also have a corresponding effect on the two-photon absorption edge at half the bandgap. Note however, that the polarization dependence of the TPA may differ slightly from the linear QCSE since $\chi^{(3)}$ (of which the imaginary part of which is responsible for TPA) is a 4th rank tensor, in contrast to the linear susceptibility (which is 2nd rank tensor).

Figure 6 shows the TPA photocurrent for a 0V bias and a +1V bias. We found that the internal quantum efficiency was essentially 100% even for small applied reverse bias fields, consistent with previous linear photocurrent measurements [19]. The physical origin of this is that the carrier escape times (for both electrons and holes) is very fast even for small applied (reverse bias) fields, and so the internal quantum efficiency will be high since the carriers escape to the contacts long before they recombine - typical carrier spontaneous recombination times are of the order of nanoseconds [24]. Only as the bias field approaches zero (near flat band conditions at +1.5 V), do the escape times increase appreciably, dropping the internal QE below 100%. The key point is that, even though the absorption mechanisms of TPA and the linear absorption may differ, once the carriers are created the dynamics that determine the internal quantum efficiency (carrier escape times versus recombination times) are identical [19,24].

In Fig. 7 we plot the external efficiency as a function of input peak power and obtain a linear relation. The external efficiency of our device was calculated according to Eq. (15), from which the slope of the linear fit of Fig. 7 was determined to be 8.6 x10^{-5} W^{-1}, seven

#106401 - $15.00 USD Received 15 Jan 2009; revised 13 Mar 2009; accepted 16 Mar 2009; published 19 Mar 2009

orders of magnitude greater than previously reported in photodiodes [13], and comparable with previously reported p-i-n waveguide devices [15]. The inclusion of quantum wells is predicted to have a large increase in the quantum efficiency, and can be theoretically close to 100% as previously shown in similar GaAs laser structures [19].

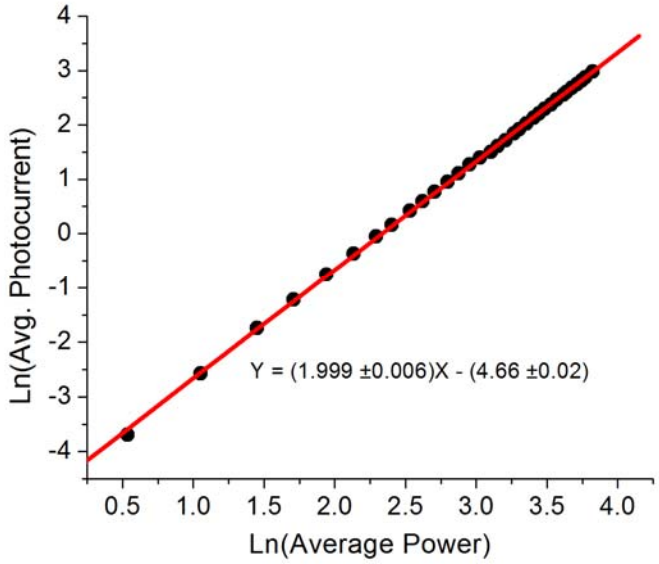

Fig. 5. Average photocurrent as a function of the input power in the waveguide. A log-log plot determines that the relation is purely quadratic, and hence that the photocurrent is a result of TPA .

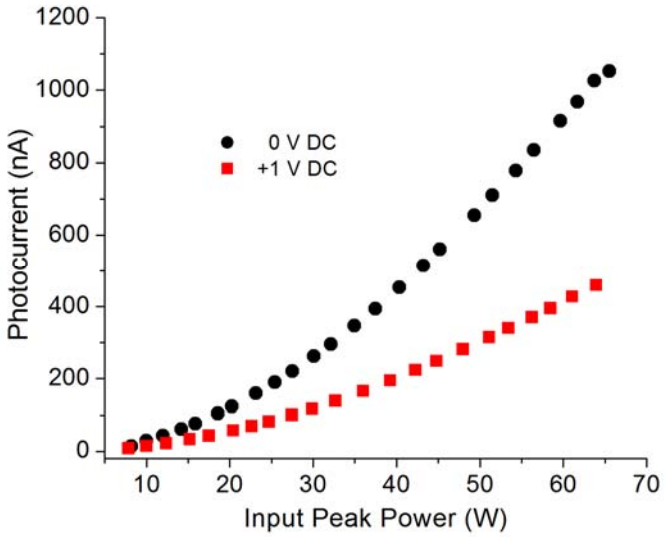

Fig. 6. Bias dependence of TPA photocurrent.

From these results it is also possible to have an estimate for the TPA coefficient. If we assume 100% internal quantum efficiency, thus neglecting non-radiative and radiative carrier recombination, we obtain $\beta \sim 0.54$ cm/GW from Eq. (18), agreeing very well with previous reports in non-MQW AlGaAs waveguides [43]. Note that typical values of the TPA coefficient in GaAs/AlGaAs waveguides are somewhat scattered with reports ranging from ~0.4 cm/GW [43], to ~10 cm/GW [30,44]. The TPA coefficient seems to depend largely on

#106401 - $15.00 USD Received 15 Jan 2009; revised 13 Mar 2009; accepted 16 Mar 2009; published 19 Mar 2009

the concentration of Al content in the core of the waveguide, as well as on how much the mode overlaps the surrounding cladding layers of the waveguide (which have a different Al content). This is understandable as an increase of the Al content increases the bandgap energy, and hence the half-badgap as well. At 15% Al content, the half-bandgap is approximately at 1550nm, and hence large variations of the TPA coefficient are to be expected for waveguide structures of various Al content in the core and cladding regions.

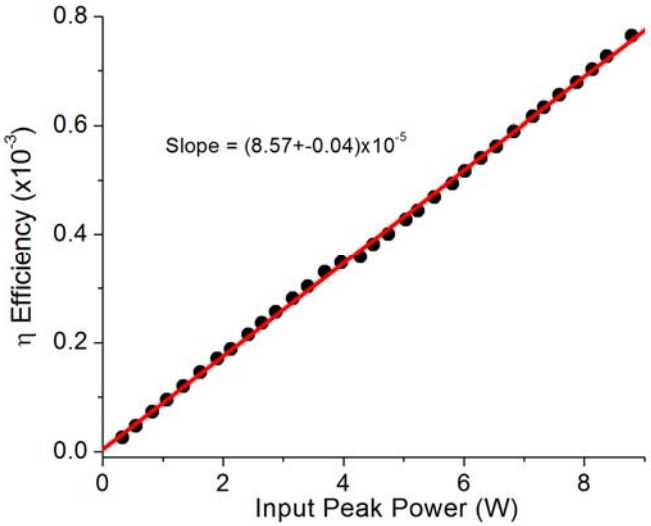

Fig. 7. External MQW device efficiency.

The minimum detectable photocurrent with our TPA photodetector, i.e. 28pA, was obtained at a peak input peak power as low as 330mW. Using Eqs. (20) and (21) we estimate the sensitivity of the device to be 0.28 mW^2 or 0.1nA/mW^2, orders of magnitude better than commercial SHG autocorrelators where ~ 10 mW^2 sensitivities (~10^{-3} nA/mW^2) are typically observed when they are coupled to photomultiplier tubes [45]. These results compare well with recent reports of SOI and InGaAsP based waveguide autocorrelators with sensitivities of 1mW^2 [46] and 0.08 mW^2 [16], respectively. Recent results in GaAs microcavities have shown a sensitivity of ~9.3 x10^{-4} mW^2 due to the TPA enhancement [7], suggesting that a highly reflective coating on our waveguide facets would significantly increase its sensitivity.

While in general the overall device sensitivity for linear waveguide photodetectors is typically very high, since the absorption length along the waveguide is much shorter than the device length (when operated above the bandgap), this is not necessarily the case for TPA detectors. For TPA detectors the absolute absorption is still typically quite small and so improving the absolute two-photon absorption – eg., by increasing the number of wells, overlap with the mode, etc. - will have a much more significant effect than for linear devices. In addition, increasing the device length would also result in larger nonlinear absorption thereby increasing the sensitivity and external efficiency of the device. Finally, as mentioned, widening the intrinsic region would decrease spurious background losses, at 1550nm, thus improving efficiency.

We note that while nonlinear photodetectors are generally quite slow since the electrical photocurrent is typically integrated (with the ultrafast operation being accomplished through the nonlinear optical response), there are applications in communications systems (such as Code Division Multiple Access, or CDMA) where it has been proposed [11] that simultaneous nonlinear detection with a fast *electrical* response time would have significant benefits. MQW waveguide photodetectors such as ours would be ideal for this, since they have been shown to be capable of ultrafast electrical response times given the appropriate fabrication (eg., planarization) processes.

#106401 - $15.00 USD Received 15 Jan 2009; revised 13 Mar 2009; accepted 16 Mar 2009; published 19 Mar 2009

Finally, looking to the future and the prospects for all-optical signal processing based on the Kerr nonlinearity in these structures [29], we note that our device has the potential to allow the direct electrical control of the nonlinear figure of merit via the quantum confined Stark Effect.

6. Conclusion

We demonstrate two-photon detection in a reverse biased GaAs MQW laser structure near 1550nm for the first time. By adjusting the wafer growth conditions we simultaneously optimize both laser and reverse biased detector performance. We observe a purely nonlinear TPA photocurrent at 1.55μm with a high sensitivity and external efficiency. The small device size, low insertion loss, high sensitivity and quantum efficiency are extremely promising for nonlinear signal processing applications such as optical performance monitoring and pulse characterization, where the benefit of low cost and ability to combining a nonlinear optical response with direct optical to electrical conversion is extremely useful. The MQW structure also raises the prospect of several qualitatively new features for TPA detectors such as a combined nonlinear optical and ultrafast electrical response, with efficient carrier sweep-out rates greatly reducing the effects of TPA generated carrier pile-up, as well as the potential for direct electrical control of the nonlinear figure of merit via the quantum confined Stark Effect.

Acknowledgments

This work was supported by the Australian Research Council (ARC) Centres of Excellence program, the FQRNT (Le Fonds Québécois de la Recherche sur la Nature et les Technologies), the Natural Sciences and Engineering Research Council of Canada (NSERC), NSERC Strategic Projects and the INRS. L.R. wishes to acknowledge a Marie Curie Outgoing International Fellowship (contract no. 040514). We are also thankful to R. Helsten for technical assistance.

#106401 - $15.00 USD Received 15 Jan 2009; revised 13 Mar 2009; accepted 16 Mar 2009; published 19 Mar 2009